AD-A090 336 AIR FORCE GEOPHYSICS LAB HANSCOM AFB MA F/G 22/1
GROUNDBASED PREDICTORS OF SPACECRAFT CHARGING DURING ECLIPSE PA--ETC(U)
MAR 80 A H WENDEL
UNCLASSIFIED AFGL-TR-80-0088 NL

1 OF 1
AD A
090336

END
DATE FILMED
11-80
DTIC

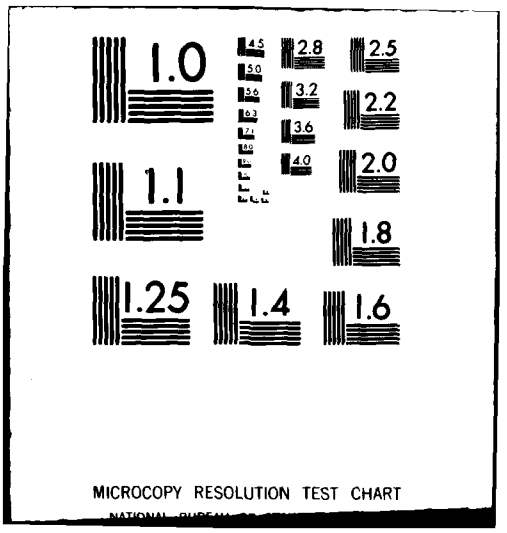
1.0
1.1
1.25
1.4
1.6
1.8
2.0
2.2
2.5
2.8
3.2
3.6
4.0
4.5
5.0
5.6
6.3
7.1
8.0
9.0
MICROCOPY RESOLUTION TEST CHART

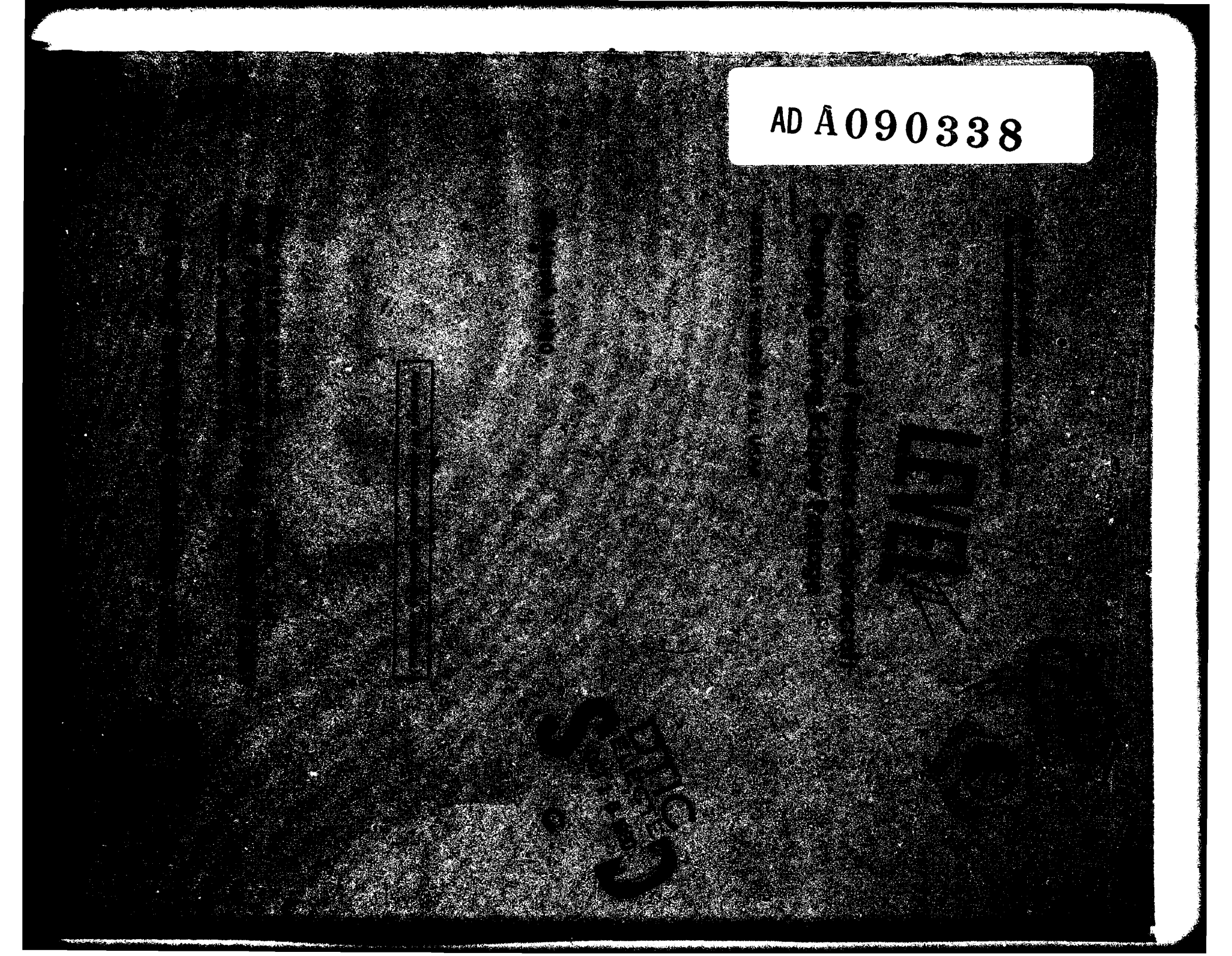

This report has been reviewed by the AFSC Information Office (OI) and is releasable to the National Technical Information Service (NTIS).

This technical report has been reviewed and is approved for publication.

FOR THE COMMANDER

Chief Technical Advisor

Qualified requestors may obtain additional copies from the Defense Technical Information Center. All others should apply to the National Technical Information Service.

(9) Air Force Surveys in Geophysics

Unclassified

SECURITY CLASSIFICATION OF THIS PAGE (When Data Entered)

REPORT DOCUMENTATION PAGE	READ INSTRUCTIONS BEFORE COMPLETING FORM
(14) 1. REPORT NUMBER AFGL-TR-80-0088 AFGL-AFSG 422 2. GOVT ACCESSION NO AD A090 338	3. RECIPIENT'S CATALOG NUMBER
(4) 4. TITLE (and Subtitle) GROUND-BASED PREDICTORS OF SPACECRAFT CHARGING DURING ECLIPSE PASSAGE	5. TYPE OF REPORT & PERIOD COVERED Scientific. Interim.
	6. PERFORMING ORG. REPORT NUMBER AFSG No. 422
(10) 7. AUTHOR(s) Arthur H. Wendel 2/Lt, USAF	8. CONTRACT OR GRANT NUMBER(s) (15) 7661 (17) 08
9. PERFORMING ORGANIZATION NAME AND ADDRESS Air Force Geophysics Laboratory (PHG) Hanscom AFB Bedford, Massachusetts 01731	10. PROGRAM ELEMENT, PROJECT, TASK AREA & WORK UNIT NUMBERS 62101F 76610803
11. CONTROLLING OFFICE NAME AND ADDRESS Air Force Geophysics Laboratory (PHG) Hanscom AFB Bedford, Massachusetts 01731	(11) 12. REPORT DATE 20 March 1980 (12) 13. NUMBER OF PAGES 21
14. MONITORING AGENCY NAME & ADDRESS(if different from Controlling Office)	15. SECURITY CLASS. (of this report) Unclassified
	15a. DECLASSIFICATION/DOWNGRADING SCHEDULE

16. DISTRIBUTION STATEMENT (of this Report)
Approved for public release; distribution unlimited.

17. DISTRIBUTION STATEMENT (of the abstract entered in Block 20, if different from Report)

18. SUPPLEMENTARY NOTES

19. KEY WORDS (Continue on reverse side if necessary and identify by block number)
Spacecraft charging
Eclipse passage
Satellite survivability

20. ABSTRACT (Continue on reverse side if necessary and identify by block number)
Much work has been done to establish the finding that spacecraft charging at geosynchronous orbit is dependent upon local plasma conditions as well as geomagnetic activity. This paper describes further verification of correlations resulting from the analysis of a large data set from the geosynchronous satellite ATS-5 during eclipse passages. In addition, ground-based geomagnetic indices were also compared with satellite potential, as well as individual magnetometer readings near the base of the geomagnetic field line nearest the satellite.

DD FORM 1 JAN 73 1473 EDITION OF 1 NOV 65 IS OBSOLETE

Unclassified

SECURITY CLASSIFICATION OF THIS PAGE (When Data Entered)

Contents

Illustrations

Tables

Ground-Based Predictors of Spacecraft Charging During Eclipse Passage

1. INTRODUCTION

1.1 Satellite Relationship to Plasma

A geosynchronous satellite in the plasmasphere remains at the plasma potential or perhaps a few volts positive potential with respect to the surrounding plasma.[1] When the satellite passes into the earth's shadow, however, the cessation of the emission of photoelectrons results in the sudden buildup of a negative charge until the potential of the satellite with respect to the plasma is up to several thousand volts negative. With such sudden high potentials, the possibility of satellite operational anomalies or physical damage due to electric arcing becomes significant. The purpose of this paper is to show relationships between the estimated potentials of the satellite just prior to, during, and after eclipse; various characteristics of the space plasma environment measured by the satellite; and diverse ground-based measurements of geomagnetic activity and local variations in the earth's magnetic field.

(Received for publication 3 March 1980)

1. Garrett, H. B., Pavel, A. L., and Hardy, D. A. (1977) Rapid Variations in Spacecraft Potential, AFGL-TR-77-0132, AD A046350, p. 11.

1.2 Spacecraft Charging

Spacecraft charging can be described in terms of the particle fluxes the spacecraft experiences while moving through the space plasma. In a plasma with electrons and positive ions (mainly protons) of roughly equal energies, the average velocity of the electrons is forty times that of protons. More electrons than protons penetrate the plasma sheath (which forms around any probe in a plasma) and impinge upon the spacecraft, resulting in an incident electron current about 100 times larger than the incident ion current. Some of the impacting electrons and ions result in the secondary emission of more electrons from the satellite, while incident electrons are also backscattered to a degree. Only the emission of large numbers of photoelectrons can counterbalance the high flux rate of these high-velocity electrons. Thus, when the spacecraft is in sunlight, the photoelectron current is responsible for the spacecraft's slight positive charge. When a spacecraft becomes shadowed, its surface no longer emits photoelectrons and becomes negatively charged to a high degree; this also holds true for the surfaces of nonrotating spacecraft permanently shadowed.

2. PROCEDURE

2.1 Selection and Analysis

Our procedure was, first, to select plasma spectrograms from which satellite potential could be estimated; that is, from those produced from data taken during the eclipse seasons (near the spring and fall equinoxes) of 1970 and 1971. Next, the first four velocity moments of the plasma energy distribution were obtained, calibrated for instrument degradation, and utilized to calculate single and two-Maxwellian charged particle currents and temperatures experienced by ATS-5. These temperatures and currents were then employed in charging models of varying complexity, yielding further estimates of satellite potential.

2.2 Magnetometer Tracings

Magnetometer tracings made at these times near the base of the geomagnetic field line associated with the satellite's position were obtained, scaled, and compared with the spacecraft's potential. All of these parameters were then subjected to multiple regression analysis by means of a straightforward matrix-inversion FORTRAN program.

3. DATA BASE

3.1 Satellite

This study is based upon data gathered by the ATS-5 satellite during 1970 and 1971. This satellite was in geosynchronous orbit near 105°W longitude with an orbital inclination of 2.30°, spinning about an axis parallel to the earth's rotational axis with a period of 0.79 sec.[2] The four spectrometers of the University of California, San Diego plasma experiment supplied the data upon which spacecraft potential estimates and plasma temperature calculations were based. Two pairs of electron and proton analyzers are described: one pair directed perpendicular to, and the other aligned parallel with the spacecraft spin axis. Both directional orientations yielded, roughly, the same results for the purpose of this study and, consequently, the average of both orientations was used.

3.2 Environment

Plasma characteristics were calculated from 10-min averages of the first four moments of the plasma distribution function described by Garrett[3] as:

the number density, $\langle n_i \rangle = 4\pi \int_0^\infty (V^0)\ f_i\ V^2\ dV = n_i$

the number flux, $\langle NF_i \rangle = \int_0^\infty (V^1)\ f_i\ V^2\ dV = \frac{n_i}{2\pi} \frac{(2\ kT_i)^{1/2}}{\pi\ m_i}$

the pressure, $\langle P_i \rangle = 4\pi \left(\frac{1}{3} m_i\right) \int_0^\infty (V^2)\ f_i\ V^2\ dV = n_i\ kT$

and the energy flux, $\langle EF_i \rangle = \left(\frac{1}{2} m_i\right) \int_0^\infty (V^3)\ f_i\ V^2\ dV = \frac{m_i n_i}{2} \frac{(2\ kT_i)^{3/2}}{\pi\ m_i}$

for particle species i.

Electron and ion currents were obtained by multiplying the appropriate number of fluxes by the charge of a single electron or proton.

Typical values were selected for these four moments as close to the entry and as close to the exit of the satellite into eclipse as possible. Sudden large particle fluxes or detector malfunctions occasionally precluded the selection of the immediately preceding or the immediately following values.

---

2. DeForest, S. E., and McIlwain, C. E. (1971) Plasma clouds in the magnetosphere, J. Geophys. Res. 76 (No. 16):3587.

3. Garrett, H. B. (1977) Modeling of the Geosynchronous Orbit Plasma Environment - Part I, AFGL-TR-77-0288, AD A053164.

A continual decrease in the value of the electron moments was observed. This is due to the decay of the electrostatic analyzers sensitivity with time. Since electron fluxes were so much higher than proton fluxes, the electron analyzers deteriorated earlier than their counterparts for positively charged particles. By the end of 1972, these electron detectors were almost totally inoperative.

To compensate for this instrument degradation, the averages of the moments during each of the four eclipse seasons (spring and fall of 1971 and 1973) were taken for both the parallel and the perpendicularly oriented devices which decayed at different rates. The moments were then normalized to yield average values comparable with the spring of 1970 for the two types of detectors.

The calibrated moments were then used to compute two different types of plasma "temperatures,"

T "average" = T_{AVG} = pressure divided by number density, and

T "root mean square" = T_{RMS} = energy flux divided by twice the number flux.

As Garrett has shown, these temperatures will be equal, and have meaning as temperatures, if and only if the plasma is a Maxwellian plasma; that is, representable by the equation:

$$f_i(V) = n_i \left(\frac{m_i}{\pi kT_i}\right)^{3/2} e^{-m V_i^2/2 kT_i}$$

where

n_i = number density of species i
m_i = mass of species i
T_i = temperature of species i
V_i = velocity of species i
K = Boltzmann constant
f = distribution in sec^3/km^6 .

The marked difference between T_{AVG} and T_{RMS} as determined from ATS-5 data is a direct result of the absence of a Maxwellian plasma at geosynchronous orbit.[4]

4. Garrett, H. B. (1978) Modeling of the Geosynchronous Plasma Environment, Proc. of the Spacecraft Charging Technology Conference-1978, AFGL-TR-79-0082/NASA Conference Publication 2071, pp. 12-14.

As further demonstrated by Garrett,[3] the actual plasma distribution function can be more successfully approximated by employing the sum of two components with different temperatures and number densities, each with a Maxwellian distribution. The electron and ion number densities and temperatures were also calculated for both of these components from the four plasma moments.

3.3 Indices and Magnetometer Data

The various geomagnetic indices considered in this study included K_p, A_p, C9, AE, AL, AU, and Dst. Most of these are described in a review paper by Rostoker.[5] The following brief description is based primarily upon this reference.

These indices are based on the averages of certain values derived from magnetometer tracings of selected stations around the world. One objective of this study was to determine whether these averaged indices or whether magnetometer tracings at the foot of the field line provided better indication of spacecraft charging.

The popular K_p index is a measure of worldwide geomagnetic activity over 3-hr periods. First, each individual station determines a K value based on the deviation between the minimum and maximum magnetometer readings along all three axes of measurement and the geomagnetic latitude of the station. The K_s index is derived by adjusting the K value to compensate for season-dependent diurnal variations in accordance with tables devised for each station. Finally, the K_s indices of a number[5] of carefully selected observatories at subauroral latitudes are averaged to yield the K_p index.

The A_p index is derived directly from K_p on a linear scale as opposed to K_p's quasi-logarithmic variation. There is a formula relating A_p to K_p for all but the highest values of K_p for which certain values are more or less arbitrarily selected.

The AL, AU and AE indices are indicators of auroral-zone magnetic activity and are calculated from magnetometer measurements of the H component from the auroral latitudes. The readings of the various stations, corrected for average value, season, and local time variation are superimposed on a single magnetogram style chart. The upper envelope of such a chart is known as AL and is determined by the maximum positive H reading for all magnetometer stations used; AU is similarly the maximum negative value of H for all observatories during a particular 2.5-min interval; AE is just the difference between these two quantities.

Further, Dst is used as an indicator of ring current strength alone and is derived from measurements of the H component of magnetic variation at several low-latitude observatories. It is basically the deviation of the H component of

---

5. Rostoker, G. (1972) Geomagnetic indices, Rev. Geophys. 10 (No. 4):935-950.

the geomagnetic field from a baseline value, adjusted for seasonal variations as well as daily solar influences.

Finally, the magnetometer tracings recorded at the Fort Churchill Observatory, Canada, located at 94.10°W longitude, 58.80°N latitude, were also used in this study. This position compares favorably with the approximate coordinates of the intersection of the geomagnetic field line nearest the ATS-5 satellite and a spherical surface 100 km above the earth: 98.8°W longitude, 55.40°N latitude. The field line tracings, made during the spring and fall of 1970 (none being available for 1971), were scaled so as to obtain an "average" level of geomagnetic activity as well as the magnitude of magnetic fluctuations in the X-direction during each of the three hours before local midnight. The average level was estimated visually, smoothing out fluctuations of short duration, and the amount of fluctuation was determined by the peak-to-peak distance between the minimum and maximum deflections within a particular hour. The average magnetometer measurements during hours 0400, 0500, and 0600 (UT) and the measurement of variation during the same hours will be referred to subsequently as M4, M5, M6, ΔM4, ΔM5, and ΔM6, respectively.

When considering various geomagnetic indices as indicators for the possibility of the accumulation of potential, one finds it useful to remember Rostoker's caveat regarding their use.[5] Due to the nonuniform distribution of magnetic observatories, and resulting lack of coverage, indices can define only the lower limit of geomagnetic activity at any particular point in time. This would be consistent with the data analyzed for ATS-5 in that charging almost always occurred when the indices reached higher levels, although not ruled out by low index values.

4. RESULTS

4.1 Estimates of Potential

Various approximate relationships between electron and ion currents measured by the satellite in sunlight, between electron and ion currents in eclipse, between electron and ion T_{AVG} and T_{RMS}, and the potential of the satellite were used to make additional estimates or predictions. These were derived from prior observation and application of elementary plasma theory. As observed, the natural logarithm of, roughly, one-tenth the electron-to-ion current ratios before eclipse was proportional to the potential buildup when multiplied by the electron temperature. This relationship was then tested with both the AVG and RMS electron temperatures as follows:

$$V_1 = T_{AVG_E} \times \ln (J_{E_o} / 10\, J_{I_o})$$

$$V_2 = T_{RMS_E} \times \ln (J_{E_o} / 10\, J_{I_o})$$

where J_{E_o} and J_{I_o} are the electron and ion currents, respectively, before the satellite enters the earth's shadow.

Garrett and Rubin also observed that, according to probe theory, when either a thick plasma sheath or no plasma sheath surrounds a spherical probe, it is negatively charged as:

$$J_E = J_{E_o}\, e^{-|qV|/T_E} \tag{1}$$

$$J_I = J_{I_o} \left(1 + \frac{|qV|}{T_I}\right) \tag{2}$$

where J_E = electron current to shadowed spacecraft

J_I = ion current to shadowed spacecraft

J_{E_o} = electron current to spacecraft before eclipse

J_{I_o} = ion current to spacecraft before eclipse

V = spacecraft potential in volts

q = unit charge such that qV is in electron volts .

Solving Eq. (1) for the potential buildup and trying both T_{AVG} and T_{RMS}, one derives the following estimates.

$$V_3 = T_{AVG} \times \ln (J_E / J_{E_o})$$

$$V_4 = T_{RMS} \times \ln (J_E / J_{E_o})$$

Equation (2) was solved for the spacecraft potential in terms of the ratio of the ion currents before and during eclipse. Again, both AVG and RMS temperatures were tested:

$$V_5 = T_{AVG} \times (1 - J_I / J_{I_o})$$

$$V_6 = T_{RMS_I} \times (1 - J_I / J_{I_o})$$

An example of the relationship observed between these predictors and the actual potentials is given in Figure 1.

When considering the usefulness of these various formulas in predicting potential buildup, one finds it useful to distinguish between two different questions which are applicable: (1) Is the potential zero or nonzero? (2) How high is the potential, given that it is nonzero? It appears that V_1, V_2, V_3, and V_4 can be applied successfully in answering both questions, whereas V_5 and V_6 are very useful in answering the first question only. In all cases, the predictors using the electron temperature data (V_1 through V_4) generally yield better results than V_5 and V_6, based on ion temperatures; V_1 and V_2, calculated using ion-to-electron current ratios before and after eclipse, seem to be better in predicting the occurrence of charging than V_3 and V_4, but are of roughly the same value in foretelling the magnitude of charging. For purposes of real-time warnings of possible charging conditions, the utilization of particle current data measured before eclipse as in V_1 and V_2 is a clear advantage, even further enhancing the usefulness of these estimates.

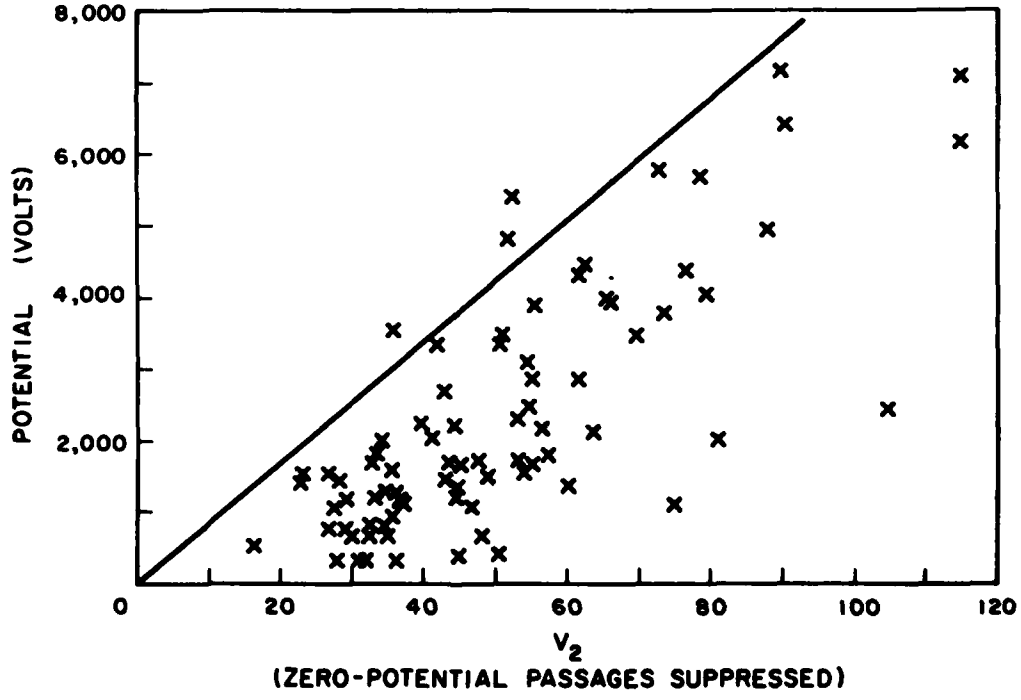

Figure 1. Distribution of RMS Electron Temperatures at Geosynchronous Orbit Measured on ATS-5, 1969-1971

Utilizing RMS, as opposed to average temperatures, for these indicators resulted in better estimates of the extent of charge accumulation only in the case of V_1 and V_2; it did not improve results for the charging/no charging determination for any of the estimates.

Finally, whereas V_5 and V_6 did not too accurately indicate the precise magnitude of the potential buildup, they appear very useful in demonstrating "safe" conditions. When these estimates yielded values of exactly zero,(that is, when there was no charge in the ion current as the satellite passed into eclipse), there was, in fact, no spacecraft charging.

One can take the technique of potential estimation by means of current balance equation $[J_E - (J_I + J_{SE} + J_{SI} + J_{BS}) = 0]$ relating the incident electron (J_E) and ion (J_I) currents with the voltage-dependent estimates for backscattered electrons (J_{BS}) as well as secondary electrons resulting from both electron (J_{SE}) and ion (J_{SI}) impacts. The photoelectron current may also be included; this was, of course, zero for the eclipse passages described here. The following table indicates the improvement in correlation with use of the more complex current-balancing estimate. This was most dramatic when the probable skewing influence of the 31 data points at zero potential was removed.

Table 1. Current-Dependent Potential Estimators

Estimator	With Zero-potential Correlation	Eclipse Uncertainty	Without Zero-potential Correlation	Eclipse Uncertainty
Single - Maximum Current	0.79	±.06	0.70	±.08
V_1	0.70	±.07	0.56	±.09
V_2	0.73	±.06	0.64	±.08
V_3	0.63	±.07	0.62	±.09
V_4	0.62	±.07	0.64	±.08
V_5	0.49	±.08	0.26	±.11
V_6	0.46	±.08	0.24	±.11

4.2 Geomagnetic Indices and Magnetometer Tracings

The indices considered and analyzed in the multiple regression were K_p, the associated A_p, and C9* for the second 3-hr period of the days (0300 to 0600 GMT) as well as AE, AL, AU, AO, and Dst for hours 0300 to 9400, 0400 to 0500, and 0500 to 0600 GMT. Also, the hourly change in Dst was explored.

*An obscure, arcane index roughly comparable to K_p.

These indices appear to divide themselves neatly into two groups: AL, Dst, and fluctuations in Dst, which showed almost no correlation with the potential, and K_p, A_p, C9, AE, and AU, which all showed moderate correlation (see Table 1). The former group of indices thus was eliminated from further calculations and intercomparisons carried out with the remaining indicators.

Again, when speaking of the relative usefulness of these indices which were considered more extensively (K_p, A_p, C9, AE4, AE5, AE6, AU4, AU5, and AU6), one can ask which are better for determining whether or not charging will occur. Further, given the occurrence of charging, one can consider which indices are better for predicting the extent of voltage buildup. For predicting the occurrence of charging, AE6, AE5, AU6, and AU5 seem to be the best indicators (with correlation coefficients of about 0.50 ± 0.08) while AE4 and AU4 and K_p have correlation coefficients which are 20 percent lower; K_p proved to be only fair as an indicator when it assumed large values, while extremely low values of K_p (0, 1-, 1+) almost always corresponded with little or no potential buildup as shown in Figure 2.

As before, the eclipses during which there was no charge buildup were eliminated, and the relationship between the potential and the indices was examined. In this case AE6 and AE5 were first; AE4, AU6, AU5, and AU4 second, and then K_p and C9. Figures 3 and 4 show potential as a function of AE6 and AU6, respectively.

It is apparent that the correlation coefficients of the sample (including eclipses without potential buildup) are significantly higher than the coefficients in the sample with the zero-potential events removed. This may be due to the uneven distribution (31 points at 0 volts).

Table 2. Correlation of Geomagnetic Indices With Spacecraft Potential

Parameter	(All Eclipses)	Uncertainty
AE6	0.57	±.10
AU6	0.55	±.10
M6	0.51	±.10
AE5	0.48	±.11
AU5	0.48	±.11
AU4	0.47	±.11
ΔM6	0.47	±.11
K_p	0.46	±.11
AE4	0.44	±.11
M5	0.43	±.11
C9	0.41	±.11
ΔM5	0.40	±.11

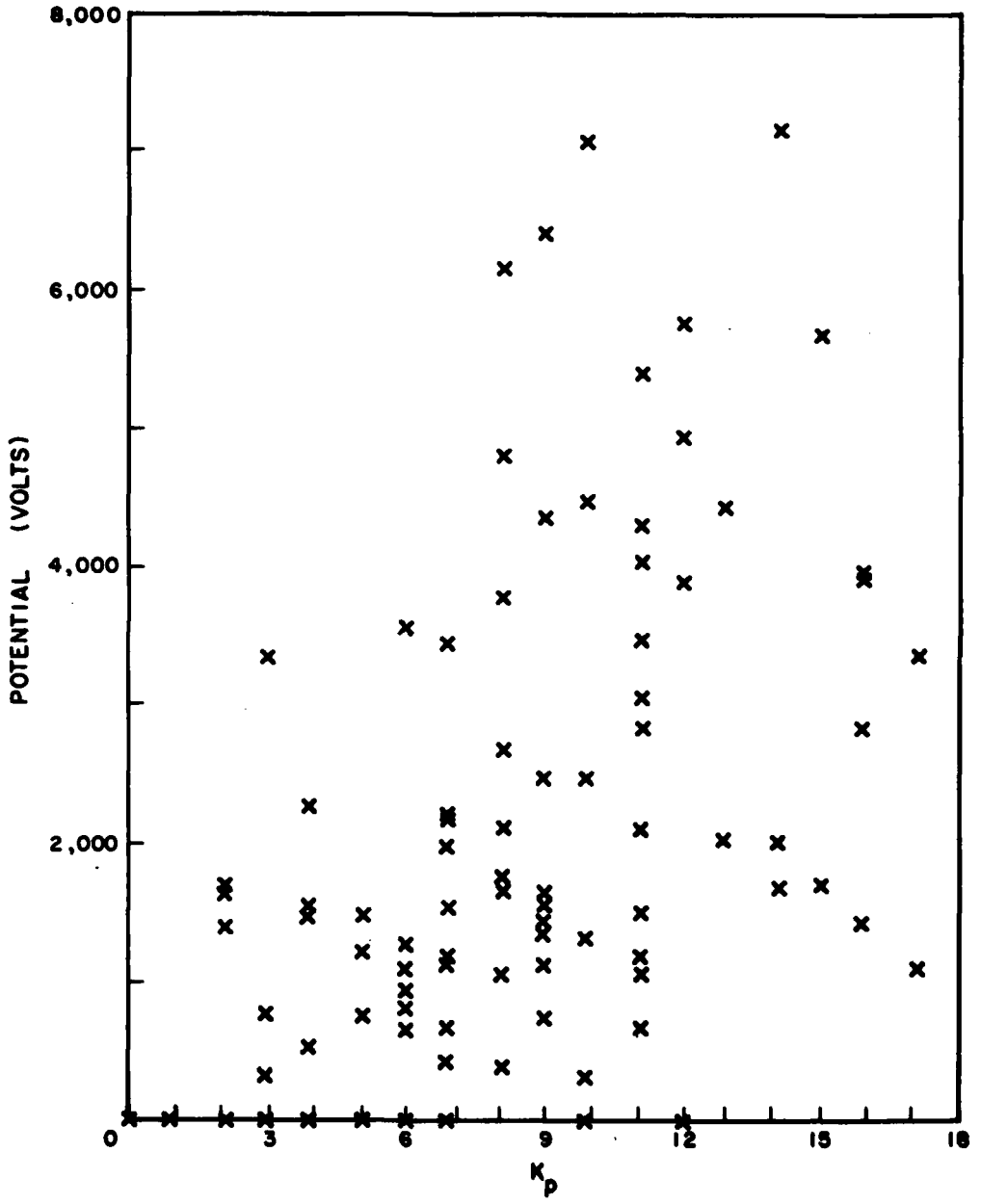

Figure 2. Distribution of RMS Ion Temperatures at Geosynchronous Orbit Measured on ATS-5, 1969-1971

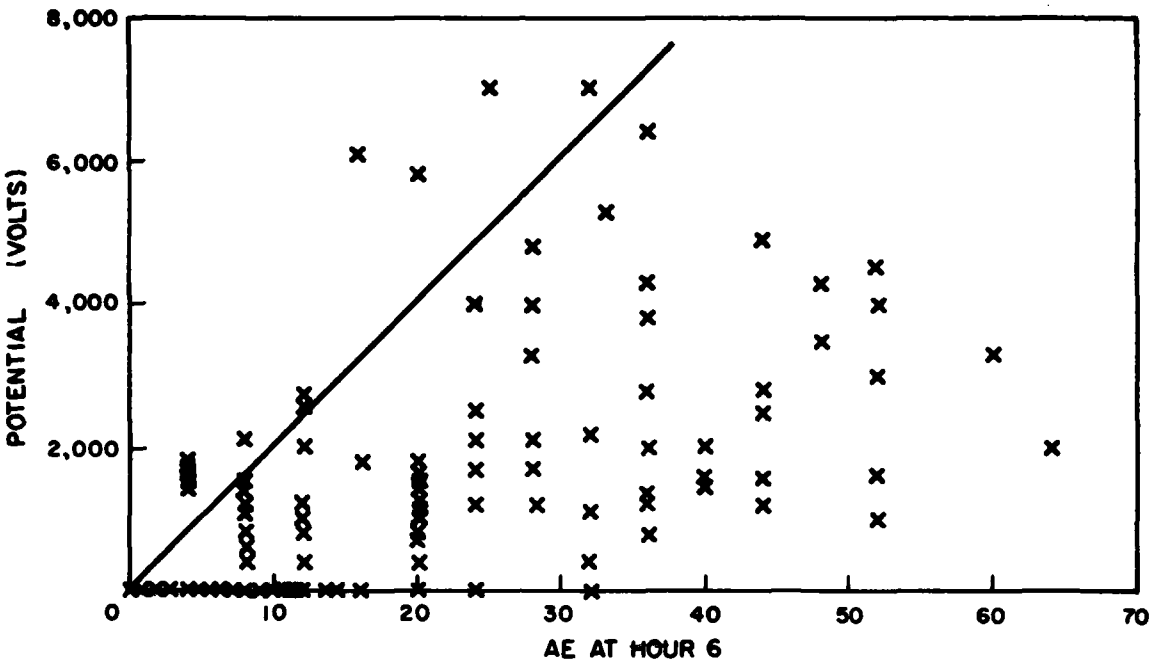

Solid line shows tendency for little or no charging when AE is low.

Figure 3. Distribution of 10-min Averages of Spacecraft Ground Potentials During Eclipse for ATS-5

When the eclipse passages without potential buildup were removed, the results were not as conclusive, owing to the small sample size. Several interesting results were noted, however, including the clear superiority of M6, followed by AU6 and AE6, the early-warning capability of AU4 (since the measurement is taken 2 hours before eclipse passage), and the relatively low correlations of potential with K_p and M4.

Table 3. Correlation of Geomagnetic Indices With Spacecraft Potential
(only eclipses in which charging occurred)

Parameter	Correlation With Spacecraft Potential	Uncertainty
M6	0.45	±.13
AU6	0.41	±.13
AE6	0.41	±.13
AU4	0.39	±.14
M5	0.36	±.14
AU5	0.35	±.14
AE5	0.33	±.14
AE4	0.31	±.14
C9	0.31	±.14
M4	0.29	±.14
K_p	0.26	±.14

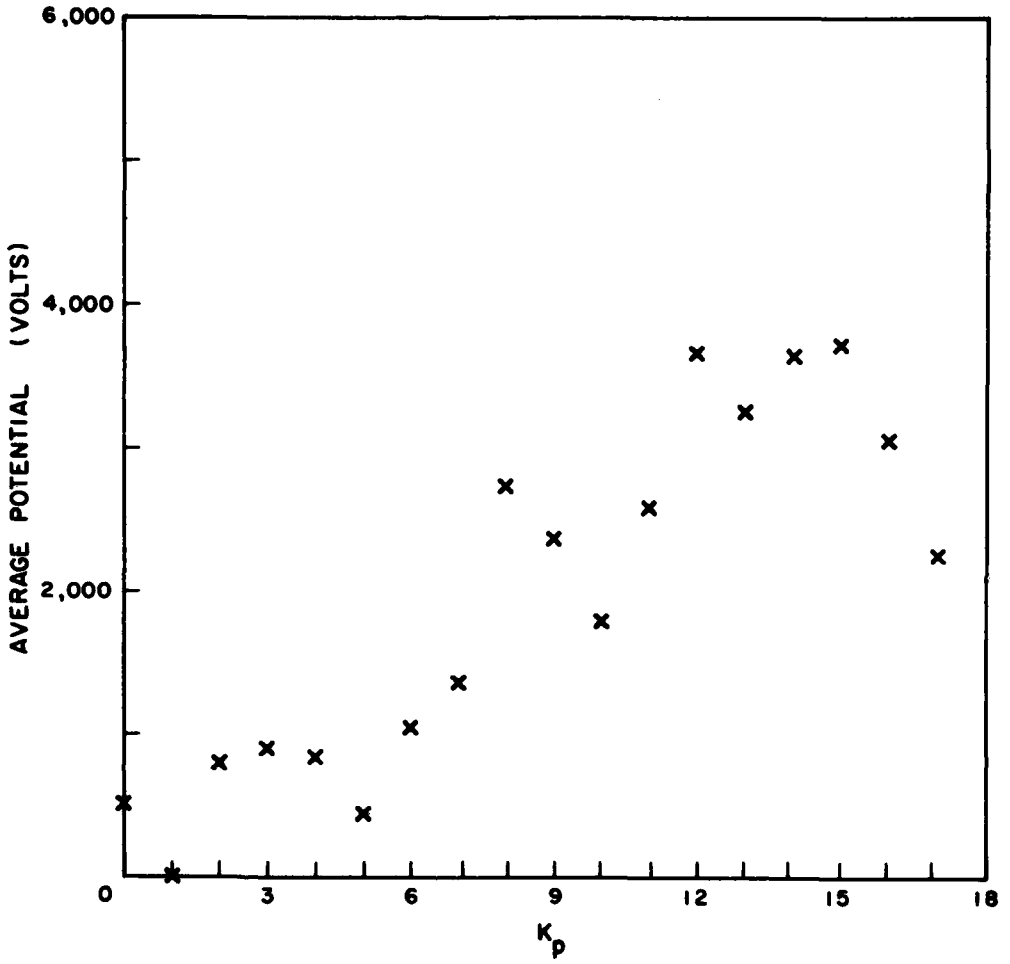

Figure 4. Distribution of Peak Spacecraft Ground Potentials During Eclipse for ATS-5

4.3 In Situ Plasma Measurements

Garrett and Rubin[6] have already considered the relationship between plasma measurements and spacecraft potential on ATS-5. In this study, close correlation was found between electron energy flux, pressure, and AVG RMS temperatures and spacecraft potential. All ion measurements showed an almost total lack of correlation. Again, the multiple regression analysis was performed both with and without zero-potential eclipse passages.

---

6. Garrett, H. B., and Rubin, A. (1978) Spacecraft charging at geosynchronous orbit - generalized solution for eclipse passage, Geophys. Res. Letters 5 (No. 10):865-878.

When the analysis was made with the zero-potential events, electron energy flux, AVG electron temperature, electron pressure, and RMS electron temperature were in good agreement with spectrogram-estimated spacecraft potential, and with electron number flux showing somewhat less correlation. Use of only the more reliable 1970 data resulted in a 10 percent increase in the correlation coefficients, but no change in the rank order of the variables as shown:

Variable (Electron)	All Data (115 points) Multiple Correlation Coefficients	Uncertainty	1970 Only (69 points) Multiple Correlation Coefficients	Uncertainty
Energy flux	0.74	±.06	0.82	±.07
TAVG	0.73	±.06	0.79	±.07
Pressure	0.67	±.07	0.76	±.08
TRMS	0.64	±.07	0.67	±.09
Number flux	0.52	±.09	0.38	±.11
Number density	0.29	±.09	0.38	±.11

When the zero-potential events are eliminated, the correlation coefficients remain relatively high, warranting greater confidence in the results. The RMS temperature is now a better correlator than the AVG temperature.

Variable (Electron)	All Data (84 points) Multiple Correlation Coefficients	Uncertainty	1970 Only (46 points) Multiple Correlation Coefficients	Uncertainty
TRMS	0.73	±.09	0.77	±.09
Energy flux	0.67	±.08	0.78	±.09
TAVG	0.62	±.09	0.72	±.10
Pressure	0.56	±.09	0.70	±.11
Number flux	0.38	±.10	0.51	±.13
Number density	0.20	±.11	0.28	±.14

The relatively low correlation coefficients of the number density were included to show an interesting tendency. We noticed that the number flux, the second velocity moment of the plasma distribution function, showed a higher correlation with potential than the first moment (number density). The third moment or "pressure" (compared with potential in Figure 5) showed greater correlation than the second, whereas the fourth moment (energy flux, as shown in Figure 6) was consistently the best correlator of the four moments. It is suggested that this is a result of the higher moments ability to measure effectively the higher energy compo-

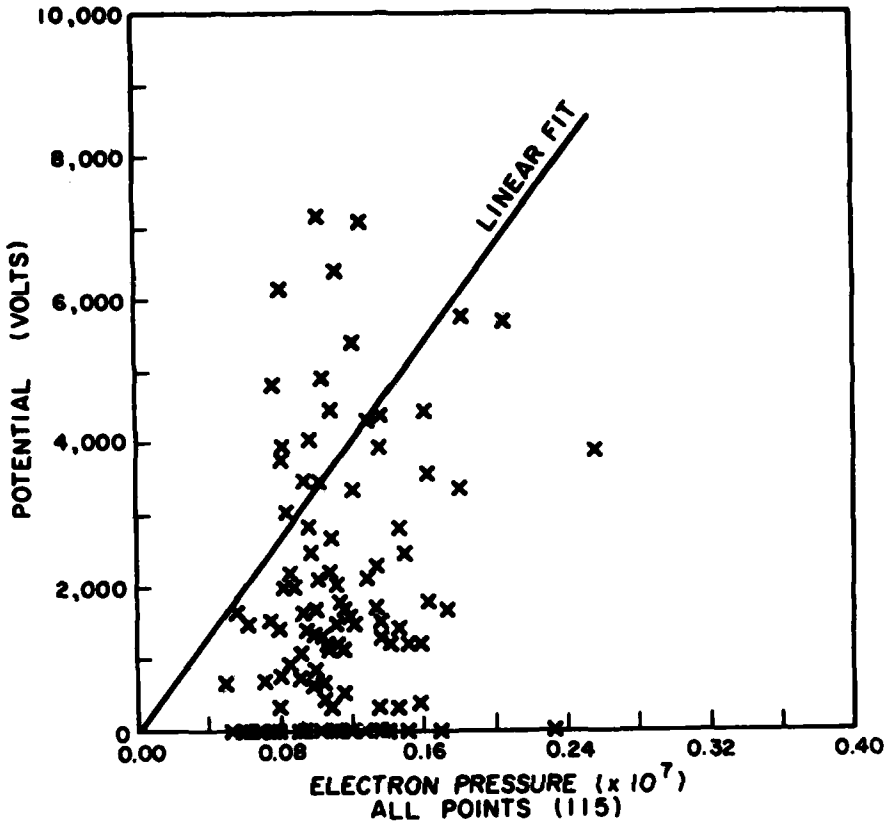

Figure 5. Distribution of Eclipse Charging Currents for ATS-5

nents of the plasma thought to be more directly responsible for spacecraft charging effects than those of lower energy.[7]

5. CONCLUSION

Clearly, among the data examined here, in situ measurements of electrons near the time of eclipse seem to be the most closely related to spacecraft charging; in fact, so much so as to make them suitable for prediction purposes. As far as the more convenient, readily available ground-based indicators are concerned,

7. Garrett, H. B., and Rubin, A. (1978) Spacecraft Charging at Geosynchronous Orbit - Solution for Eclipse Passage, AFGL-TR-78-0122, AD A058983.

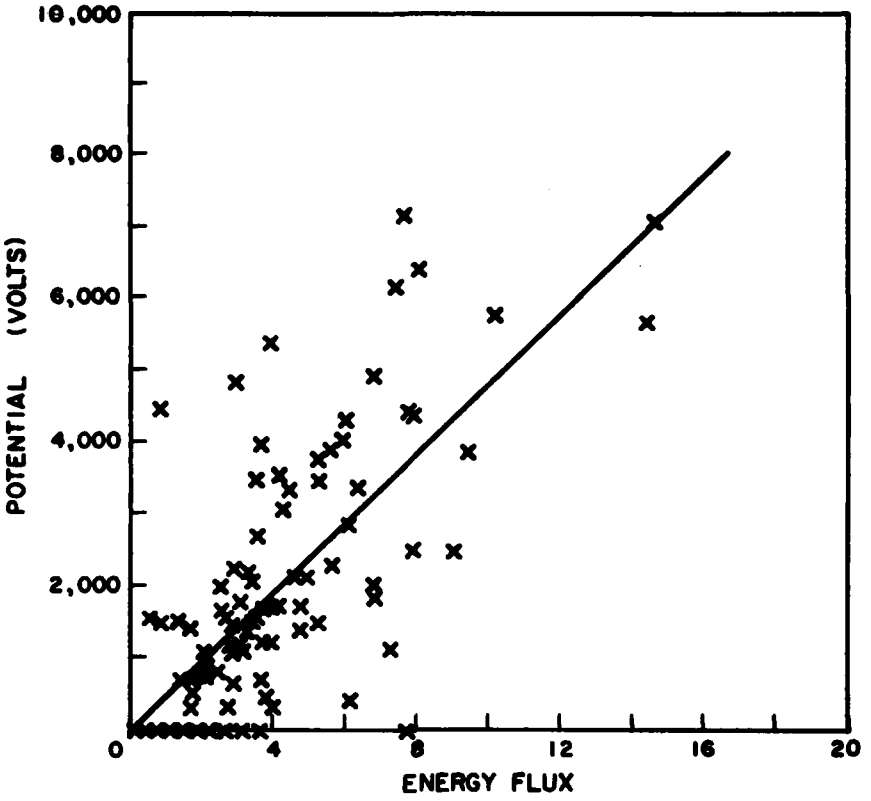

Figure 6. Dependence of ATS-5 Ground Potential on RMS Plasma Electron Temperature

AE, AU, and the local magnetometer readings at the base of the field line seem to be the best candidates. While the relationship between these parameters and potential buildup was not as direct as the in situ measurements, further comparisons will be made using the superior ATS-6 and SCATHA data which will, it is hoped, show a more direct correlation.

Furthermore, higher moments of the plasma distribution function will be calculated from this more recent data, in order to determine if the higher energy plasma components thus isolated are more directly related to spacecraft charging.

References

1. Garrett, H. B., Pavel, A. L., and Hardy, D. A. (1977) Rapid Variations in Spacecraft Potential, AFGL-TR-77, AD A046350, p. 11.
2. DeForest, S. E., and McIlwain, C. E. (1971) Plasma clouds in the magnetosphere, J. Geophys. Res. 76 (No. 16):3587.
3. Garrett, H. B. (1977) Modeling of the Geosynchronous Orbit Plasma Environment - Part I, AFGL-TR-0288, AD A053164, p. 10.
4. Garrett, H. B. (1978) Modeling of the Geosynchronous Plasma Environment, Proc. of the Spacecraft Charging Technology Conference - 1978, AFGL-TR-79-0082/NASA Conference Publication 2071, pp. 12-14.
5. Rostoker, G. (1972) Geomagnetic indices, Rev. Geophys. 10 (No. 4):935-950.
6. Garrett, H. B., and Rubin, A. (1978) Spacecraft charging at geosynchronous orbit - generalized solution for eclipse passage, Geophys. Res. Letters 5 (No. 10):865-878.
7. Garrett, H. B., and Rubin, A. (1978) Spacecraft Charging at Geosynchronous Orbit - Solution for Eclipse Passage, AFGL-TR-78-0122, AD A058983.